Science of the Total Environment 857 (2023) 159326

Contents lists available at ScienceDirect

Science of the Total Environment

journal homepage: www.elsevier.com/locate/scitotenv

A simple SEIR-V model to estimate COVID-19 prevalence and predict SARS-CoV-2 transmission using wastewater-based surveillance data

Tin Phan [a,1], Samantha Brozak [b,1], Bruce Pell [c], Anna Gitter [d], Amy Xiao [e], Kristina D. Mena [d], Yang Kuang [b,*], Fuqing Wu [d,*]

[a] Theoretical Biology and Biophysics Group, Los Alamos National Laboratory, NM, USA
[b] School of Mathematical and Statistical Sciences, Arizona State University, AZ, USA
[c] Department of Mathematics and Computer Science, Lawrence Technological University, MI, USA
[d] The University of Texas Health Science Center at Houston, School of Public Health, Houston, TX, USA 77030
[e] Center for Microbiome Informatics and Therapeutics; Department of Biological Engineering, Massachusetts Institute of Technology

HIGHLIGHTS

- A simple and effective framework is developed to bridge WBS and epidemic model.
- SEIR-V model recapitulates the temporal dynamics of viral load in wastewater.
- Model predicts the number of COVID-19 case peaked earlier and higher than reported data.
- Incorporating viral decay in wastewater improves model performance and robustness.

GRAPHICAL ABSTRACT

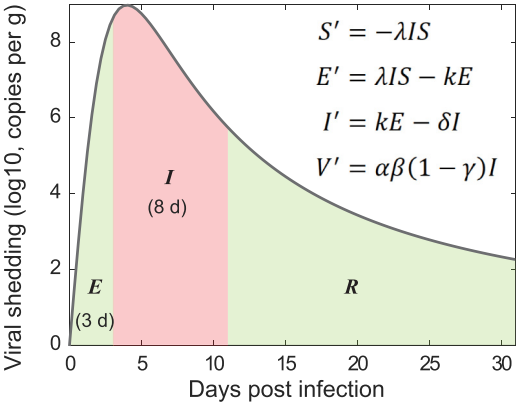

ARTICLE INFO

Editor: Damià Barceló

Keywords:
SEIR-V model
Wastewater-based epidemiology
Epidemic model
SARS-CoV-2
Temperature

ABSTRACT

Wastewater-based surveillance (WBS) has been widely used as a public health tool to monitor SARS-CoV-2 transmission. However, epidemiological inference from WBS data remains understudied and limits its application. In this study, we have established a quantitative framework to estimate COVID-19 prevalence and predict SARS-CoV-2 transmission through integrating WBS data into an SEIR-V model. We conceptually divide the individual-level viral shedding course into exposed, infectious, and recovery phases as an analogy to the compartments in a population-level SEIR model. We demonstrated that the effect of temperature on viral losses in the sewer can be straightforwardly incorporated in our framework. Using WBS data from the second wave of the pandemic (Oct 02, 2020–Jan 25, 2021) in the Greater Boston area, we showed that the SEIR-V model successfully recapitulates the temporal dynamics of viral load in wastewater and predicts the true number of cases peaked earlier and higher than the number of reported cases by 6–16 days and 8.3–10.2 folds ($R = 0.93$). This work showcases a simple yet effective method to bridge WBS and quantitative epidemiological modeling to estimate the prevalence and transmission of SARS-CoV-2 in the sewershed, which could facilitate the application of wastewater surveillance of infectious diseases for epidemiological inference and inform public health actions.

* Corresponding authors.
E-mail addresses: kuang@asu.edu (Y. Kuang), fuqing.wu@uth.tmc.edu (F. Wu).
[1] These authors contribute equally

http://dx.doi.org/10.1016/j.scitotenv.2022.159326
Received 19 July 2022; Received in revised form 15 September 2022; Accepted 5 October 2022
Available online 8 October 2022

1. Introduction

Wastewater-based surveillance (WBS) has been used as a public health tool to monitor SARS-CoV-2 infection in the population since the beginning of the COVID-19 pandemic. So far, WBS has been widely implemented in over 67 countries (Naughton et al., 2021). The Centers for Disease Control and Prevention (CDC) also launched the National Wastewater Surveillance System in late 2020 to monitor the spread of COVID-19 in the United States (CDC, 2020). Wastewater pools SARS-CoV-2 particles excreted by infected individuals irrespective of clinical symptoms or presentation, which provides an opportunity to capture the viral shedding prior to symptoms and estimate the true magnitude of viral infections in communities (Bivins et al., 2020; Hart and Halden, 2020; Peccia et al., 2020; Randazzo et al., 2020; Saguti et al., 2021; Wu et al., 2022b). Previous work has shown that SARS-CoV-2 concentrations in wastewater were much higher than expected from clinically reported cases and preceded clinically reported data by 4–10 days (Wu et al., 2020, 2022b; Peccia et al., 2020), and up to 14 days (Krivoňáková et al., 2021; Karthikeyan et al., 2022). Furthermore, the fast turnaround time of wastewater and flexible sampling strategy enable WBS to provide a near real-time monitoring of viral transmission in the sewershed. Finally, WBS is less resource intensive than the large-scale, individual-based clinical testing and thus can be used as a cost-efficient tool for monitor the trend of viral infection in the population and new variants when combined with next-generation sequencing (Bivins et al., 2020; Safford et al., 2022; Wu et al., 2022a). These properties make WBS a feasible public health tool to monitor SARS-CoV-2 in an endemic, which can also be customized for future pandemics.

WBS has enabled researchers to estimate the total viral load in a sewershed; however, there are still limitations regarding quantifying and predicting viral transmission in a community. Few recent studies have tried to build classical susceptible-infected-removed (SIR)-type models to bridge the measured viral concentration and reported case number. For example, Proverbio et al. (2022) added a variable that keeps track of actively shedding individuals in a stochastic susceptible-exposed-infectious-recovered (SEIR) model and used a constant viral shedding rate to connect the number of infected cases to viral concentration in wastewater (Proverbio et al., 2022). Conversely, Brouwer et al. (2022) accounted for time dependent viral shedding rates by incorporating multiple subclasses with different shedding rates within each infected stage of the model to better predict viral concentrations and reported cases (Brouwer et al., 2022). A similar approach is conducted by Nourbakhsh et al. (2022), but with more sub-classification of the infected class (Nourbakhsh et al., 2022). These modeling approaches allow the modelers to connect viral concentrations in wastewater with the reported cases and predict the course of the pandemic.

Dynamical models in epidemiology often overlook the opportunity to utilize biologically interpretable and experimentally measurable parameters in the link between infected people and the shed viral RNA in wastewater. The model structure is usually complicated with many parameters, so it is difficult to fully parametrize the models without running into issues such as model identifiability. Hence, our primary objective in this work is to leverage our understanding of the biology of SARS-CoV-2 shedding to construct a simple, mechanistic, dynamic model that connects viral load in wastewater with the total number of infected cases in the sewershed. Our secondary objective is to introduce the effect of wastewater temperature into the modeling framework due to its significant impact on the viral loss (or decay) rate in the sewer (Hart and Halden, 2020).

2. Materials and methods

2.1. Samples and wastewater data

Raw, 24-h composite wastewater samples were collected from the Deer Island wastewater treatment plant in Massachusetts from October 02, 2020 to January 25, 2021. The Massachusetts wastewater treatment plant where we obtained samples has two major influent streams, which are referred to as the "northern" and "southern" influents. The daily flow rates during the sampling period for the northern and southern influents are 4.54e5–2.3e6 m^3/day, and 2.16e5–1.19e6m^3/day, respectively. Together the two catchments represent approximately 2.3 million wastewater customers in Middlesex, Norfolk, and Suffolk counties, primarily in urban and suburban neighborhoods. There are 5100 miles of local sewers transporting wastewater into 227 miles of interceptor pipes to the wastewater treatment plant (www.mwra.com), and the typical turnaround time for the plant to treat wastewater is 24 h. Samples were processed as they were received. Experimental methods and data were reported in our previous work (Wu et al., 2022b; Xiao et al., 2022). Briefly, the samples were pasteurized at 60 °C for 1 h for disinfection, and then filtered with 0.2 μm hydrophilic polyethersulfone membrane (Millipore Sigma) to remove bacterial cells and debris. Then, 15-ml filtrate was concentrated to ~200 ul with Amicon Ultra Centrifugal Filter (30-kDa cutoff, Millipore Sigma), and lysed with Qiagen AVL buffer followed by RNA extraction with Qiagen RNeasy kit. SARS-CoV-2 concentrations were quantified by one-step reverse transcription-polymerase chain reaction (RT-PCR) with the Taqman Fast Virus 1-Step Master Mix (Thermofisher) and CDC N1 and N2 primers/probes. Ct values were transformed to copies per ml of wastewater using standard curves for N1 and N2 targets established with synthetic SARS-CoV-2 RNA (Twist Bioscience) as the template. To compute the total viral load in the sewershed, we first averaged the viral concentration in the northern and southern influents by the sampling date, which is then multiplied by the total influent flow rates (i.e., sum of flow rates of northern and southern influents) on the same day.

2.2. Clinical data source

The clinical COVID-19 case data for Norfolk, Suffolk, and Middlesex Counties served by the Massachusetts wastewater treatment plant were downloaded from Massachusetts government website (www.mass.gov). The plant covers about 71.9 % of the total population in the three counties, including almost all of Suffolk County (99.8 %), 59.8 % of Middlesex County, and 68.7 % of Norfolk County, based on the 2020 Census population data. For simplicity, we summed the number of clinical cases from each county to represent the total cases in the catchment of the wastewater treatment plant, which is used to compare with the modeling results. Temporal fecal viral shedding data from COVID-19 patients were kindly provided by (Wölfel et al., 2020).

2.3. Relationship between wastewater viral concentrations and infectious cases

Assuming we can obtain the fecal viral shedding distribution function over time, we can approximate a constant rate of fecal viral shedding over the duration of infectiousness. In this way, the viral RNA production is proportional to the number of people in the infectious compartment I of the SEIR model. That is:

$$\text{total viral production in wastewater} \approx \alpha \times \beta \times (1-\gamma) \times I, \tag{1}$$

where the proportional constant is defined based on biological parameters similar to (Saththasivam et al., 2021): α is the fecal load with unit g/day/person, β is the viral shedding rate in stool with unit viral copies/g, and γ is the fraction of viral loss in the sewer.

2.4. Approximation of fecal viral shedding profile

A key component of this approach is the generation of fecal viral shedding profile. Let $f(t)$ be the function that describes the temporal fecal viral shedding profile. Upon infection, the shedding of virus in stool should be very small, then reaches a peak before decreasing to 0. Mathematically, this means $f(0) = 0$, $\lim_{t\to\infty} f(t) = 0$ and $f(t)$ has a unique maximum for some $t > 0$. While beta and gamma functions are often used to represent $f(t)$ (Wu et al., 2022a; Ferretti et al., 2020; He et al., 2020), we introduce a

phenomenological function $f(t)$ that is more tractable than the standard beta and gamma functions:

$$f(t) = \frac{\omega_1 t}{\omega_2^2 + t^2}. \quad (2)$$

In this form, ω_1 is a magnitude modifier parameter ($\log_{10}$ *viral RNA copy per g per day*) and ω_2 (*day*) represents the timing for peak viral shedding and influences the timing and the magnitude of the peak of the viral shedding profile. Specifically, $f(t)$ peaks at $\frac{\omega_1}{2\omega_2}$ when $t = \omega_2$. Thus, if the peak timing and magnitude of the viral shedding profile are known, then $f(t)$ can be uniquely defined. It is necessary to mention that $f(t)$ is the overall viral shedding into the wastewater from infected individuals; however, it mostly means fecal shedding in this work. We did not include the viral shedding from urine or other sources (sputum or saliva) because previous studies showed that no or low level of virus was detected in urine samples of typical patients despite high viral load (Wölfel et al., 2020; Jones et al., 2020), and the total amount of virus in sputum or saliva are likely to be insignificant compared to stool due to the huge difference in volume.

2.5. Simple wastewater epidemiological model

$$\begin{aligned} S' &= -\lambda IS \\ E' &= \lambda IS - kE \\ I' &= kE - \delta I \\ V' &= \alpha\beta(1-\gamma)I \end{aligned} \quad (3)$$

In this model, S denotes the susceptible population, E is the infected but yet to be infectious population (or the exposed class), I is the infectious class, and V is the cumulative viral load in wastewater. The R compartment (recovered individuals) does not contribute to the transmission dynamics in the SEIR model, hence omitted here. Susceptible people are infected by the infectious class at a rate λI. Exposed individuals become infectious at a rate k. Infectious individuals recover at a rate δ and shed virus at a rate $\alpha \times \beta$, where α is the fecal load and β is the average viral shedding rate in Eq. (1). The time spent in the E and I classes are exponentially distributed with average duration of $1/k$ and $1/\delta$, respectively. γ is the viral degradation and loss rate in the sewer pipes, so only a fraction $(1-\gamma)$ of virus is detected in the wastewater sample. The expression for V follows directly from Eq. (1).

Several studies note that infectious virus is detectable in nose and throat swabs only when the total viral load is above 10^{5-6} copies/mL (Killingley et al., 2022; Ke et al., 2021; Wölfel et al., 2020; Kampen et al., 2021). Since a certain level of infectious viruses is required for disease transmission, this implies that the infectious period does not start until the viral load (within host) reaches above 10^{5-6} virus copies/mL. The shedding of infectious virus that links to transmission happens early and rapidly diminishes within 10 days after symptom onset; however, significant heterogeneity exists (Ke et al., 2022; Heitzman-Breen and Ciupe, 2022; Boucau et al., 2022). This agrees with previous observations that viral loads above 10^6 copies/mL are associated with a high probability of transmission (Ke et al., 2021). Together, these observations suggest that in this SEIR epidemic model, we can separate the exposed class (E) based on the duration before viral load reaches 10^{5-6} copies/mL, and the infectious class (I) based on the duration that viral load stays above 10^{5-6} copies/mL. This results in an incubation period of about 3 days and an infectious period of 8 days based on the viral dynamics profile in the SARS-CoV-2 Human Challenge experiment in healthy young adults (Killingley et al., 2022). These estimates are within previous estimated ranges of 2–7 days for incubation periods (Li et al., 2020; Lauer et al., 2020; Guan et al., 2020) and consistent with the updated guideline from CDC where the average infectious duration is about 2 days before and 8 days after symptom onset (CDC, 2022a). Thus, we fix the average exposed duration to 3 days, which is equivalent to fixing $k = \frac{1}{3}$ per day (Fig. 1A). Similarly, we fix the average infectious duration to 8 days, which is equivalent to fixing $\delta = \frac{1}{8}$ per day. Thus, in our model, parameters λ, α, β, and γ need to be estimated.

By fitting the model to wastewater data covering the second wave of the pandemic, specifically, from Oct 2 to Dec 16, 2020, we can approximate the susceptible (to an emerging variant) to be the entire population served by the wastewater treatment plant. For simplification, we assume that there are no infectious individuals initially ($I(0) = 0$), only infected individuals ($E(0) > 0$) due to the assumed lack of immunity to new circulating variants. The initial value for the virus concentration in wastewater can be taken from the first data point. Thus, $E(0)$ is the only unknown initial condition.

The parameters and initial conditions that remain to be estimated are: λ, α, β, γ, and $E(0)$. Since the viral production rate is $\alpha\beta(1-\gamma)$, and we only have viral concentration (or total viral load) data, it is impossible to estimate a unique set of values, or specific values, for α, β, *and* γ. For example, the product of $\alpha = 1, \beta = 2, \gamma = 0.5$ is the same as when $\alpha = 10, \beta = 1, \gamma = 0.9$. This reflects the pertinent issue of model identifiability in mathematical models in biology and epidemiology (Tuncer et al., 2022; Eisenberg et al., 2013; Wu et al., 2019; Ciupe and Tuncer, 2022). Thus, an important step in our approach is the direct estimations of β and γ, which would allow us to identify α uniquely.

2.6. Incorporating the effect of temperature on the viral degradation rate

In order to account for temperature variation over time, a sine curve was fit to the average of temperatures at the northern and southern influents (Brozak et al., 2022). The curve describing the temperature in degrees Celsius at time t (Fig. S1) is given by

$$T(t) = 3.6249 \ \sin(0.0202t - 4.4665) + 16.2298.$$

The temperature-adjusted half-life is described by

$$\eta(T) = \eta_0 Q_{10}^{-(T(t)-T_0)/10\ ^\circ C}, \quad (4)$$

where η_0 is the half-life in hours at ambient temperature T_0 and Q_{10} is the temperature-dependent rate of change (McMahan et al., 2021; Hart and Halden, 2020). Q_{10} is typically between 2 and 3 for biological systems, and assumed here to be 2.5 (Bˇehrádek, 1930; Reyes et al., 2008).

The temperature-adjusted first-order decay rate $\xi(T)$ (per hour) is then

$$\xi(T) = \frac{\ln 2}{\eta(T)}.$$

We used the simple exponential decay equation $V' = -\widehat{\eta}(T)V$ to estimate the losses in the sewer γ. Then,

$$V(t) = V_0 e^{-\xi(T)t}, \quad (5)$$

where V_0 is the amount of viral RNA in the sewers at time $t = 0$. Thus, the amount of virus that arrives to the wastewater treatment plant is

$$V(t_{arrive}) = V_0 e^{-\xi(T)t_{arrive}}, \quad (6)$$

where t_{arrive} is the time it takes the viral RNA to travel to the wastewater treatment plant after excretion. The amount of virus lost is given by $V_0 - V(t_{arrive})$. Thus, the proportion of viral RNA lost in the sewer is given by

$$\gamma(T) = \frac{V_0 - V(t_{arrive})}{V_0} = 1 - \frac{V(t_{arrive})}{V_0} = 1 - e^{-\xi(T)t_{arrive}}, \quad (7)$$

where the last equality follows from Eq. (6). We provide estimates of the die-off fraction under various scenarios in Table S3 (Supplementary Material). Note that $\gamma(T)$ varies with temperature over the course of fitting and forecasting.

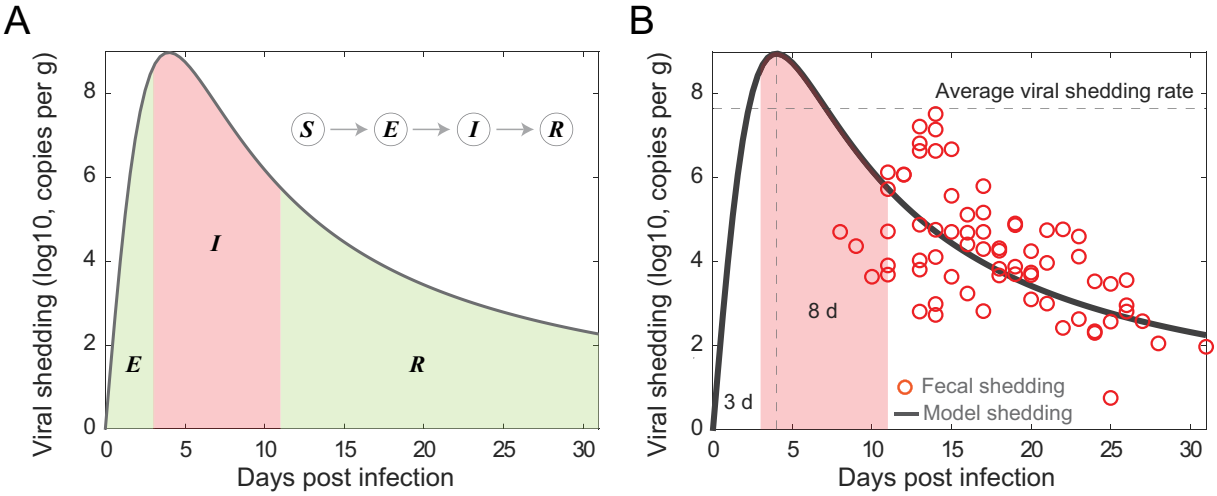

Fig. 1. Illustration and fitting fecal viral shedding dynamics. (A) Illustration of the fecal viral shedding dynamics based on the infection progression. The viral shedding profile is divided into three periods shaded: Exposed (*E*), Infectious (*I*), and Recovered (*R*). The red-shaded region is the period of infectiousness *I*, which is corresponding to the compartment *I* in the SEIR model. (B) Fitting of the proposed viral shedding function to viral shedding in hospitalized patients' stool data from (Wolfel et al. 2020). While aggregated data seem to show a viral shedding peak at around day 13–14, declining trends were found in the 9 individual cases. The average viral shedding rate in stool during the infectious period (from day 3 to day 11) is 4.49×10^7 viral RNA per g. The horizontal dashed line is the average fecal viral shedding rate for infectious individuals inferred from the model. The viral shedding peak is set at the 4th day post infection.

2.7. Data fitting

Our goal is to fit the SEIR-V model to viral concentration in wastewater data to infer the true number of cases. Then, we compare the predicted number of cases with the daily reported case data. In our model, the variable V is the cumulative viral load in wastewater. Thus, the difference of V in every 24-hour period reflects the daily measurement data of total virus concentration in wastewater. To reflect this observation, we aim to minimize the sum of square error (SSE_V) between these two quantities in our fitting. Hence, our minimization objective is:

$$SSE_V = \Sigma_{t_d}\left(\log\left(\int_{t_d-1}^{t_d} V'(s)ds\right) - \log\left(\hat{V}(t_d)\right)\right)^2. \quad (8)$$

Here, $\widehat{V}(t_d)$ is the total virus concentration experimentally measured on day t_d, which equals to viral RNA concentration in wastewater (C_{RNA}) multiplied by the total flow (F) data. $\int_{t_d-1}^{t_d} V'(s)ds$ is the corresponding quantity in our model. Once we obtain a reasonable fit to the data, the inferred number of true cases is given by:

$$\textit{Daily case number} = C_{\textit{cumulative cases}}(t_d) - C_{\textit{cumulative cases}}(t_d - 1), \quad (9)$$

where $C_{cumulative\ cases}(t)$ is a variable that keeps track of the cumulative infected cases, e.g., $C_{cumulative\ cases}' = \lambda IS$.

For the minimization algorithm, we use MATLAB function *fmincon* and *multistart*. Similarly, the fecal viral shedding function is fitted by minimizing the objective function SSE_f:

$$SSE_f = \Sigma_{t_n}\left(f(t_n) - \widehat{f}(t_n)\right)^2, \quad (10)$$

where $\widehat{f}(t_n)$ is the fecal shedding data at day t_n. Note that, we assume reported data represents a single time point, which is equivalent to assuming the viral shedding is approximately constant over the course of one day. A more technical approach would be to integrate $f(t)$ similar to Eq. (8), then average it to compare with $\widehat{f}(t_n)$. Instead, here we pass the integration to the average stool shed per day (α), and the average viral shedding over one day is given by ($\alpha \times \beta$) during the infectious period.

3. Result

3.1. Determining the average fecal viral shedding rate in infectious period

We observed that there is a striking similarity in the viral load profiles for the nose, throat, and stool for infected individuals from the time of infection to recovery qualitatively (Wölfel et al., 2020, Killingley et al., 2022, Van Kampen et al., 2021). In all three cases, high viral load/shedding is associated with the infectious duration of the infection. This observation suggests that in the classical SEIR epidemic model, we can make the simplifying assumption that the infectious individuals contribute substantially to the viral pools in wastewater. As illustrated in Fig. 1A, the viral shedding profile is divided into three periods shaded: Exposed (*E*), Infectious (*I*), and Recovered (*R*). With this framework, we can approximate the viral load in wastewater using the viral shedding from the infectious population. Furthermore, we can estimate the average viral shedding rate based on the viral shedding function $f(t)$ and the fixed average duration of infectiousness (see Materials and Methods).

Fig. 1B shows the best fit of the model to the fecal viral shedding rate data in Wölfel et al. (Wölfel et al., 2020). We assumed five days from infection to symptom onset in the fecal viral shedding data, which is in range of 2–14 days estimated for the general population (CDC, 2022b; Lauer et al., 2020). Furthermore, we fixed the viral peak at day four ($\omega_2 = 4\ day$). There is no well-established timing of the peak fecal viral shedding rate; however, the peak time for viral load in nose and throat is around 4.7 and 6.2 days after inoculation, respectively (Killingley et al., 2022), and maybe even earlier in stool (Wu et al., 2022a). The best fit parameter is $\omega_1 = 71.97\ \log_{10}\ viral\ RNA\ copy\ per\ g\ day$. Using the best fit, we estimate the average fecal viral shedding rate for an infectious individual to be:

$$\beta = \frac{1}{11-3}\int_3^{11} f(t)dt = \frac{1}{8}\int_3^{11} \frac{71.97t}{16+t^2}dt \approx 7.65\ \log_{10}\text{viral RNA per g} \quad (11)$$

A conversion gives:

$$\beta = 4.49 \times 10^7 \text{ viral RNA per g}. \quad (12)$$

This number is close to the measured median viral RNA load $10^{7.68}$ (ranging from $10^{4.1}$ to $10^{10.27}$) copies/ml in infected individuals in South Korea (Han et al., 2020), and the extrapolated fecal shedding rate of

$10^{7.30}$ (ranging from $10^{5.74} - 10^{8.28}$) copies/g of 711 infected individuals in the dormitories at University of Arizona (Schmitz et al., 2021). Thus, we fixed fecal viral shedding rate β in our SEIR-V model to this value.

3.2. SEIR-V model captures the temporal dynamics of clinical COVID-19 cases

We developed an SEIR-V model to understand SARS-CoV-2 transmission using WBS data in the second wave of the pandemic and the computed average fecal viral shedding rate during the period of infectiousness. Fig. 2 shows the best fit and its inference with parameter values and possible ranges summarized in Table 1. We fitted the model to total viral RNA copies in wastewater data up to the grey dashed line (December 18, 2020), then simulated the model out to January 25, 2021, see Fig. 2A. The fitting region was chosen before the peak in the viral RNA data, so that we could test the model's prediction of the peak against the data. Additionally, the fitting region from October 02, 2020 to December 18, 2020 potentially limits the influence from vaccination and the emergence of the alpha variant, which began near the end of 2020.

Using the best fit parameters, we computed the number of new cases and compared it to the reported cases. As shown in Fig. 2B, the model simulation recapitulates the trend of clinically reported daily new cases and predicts an earlier and higher peak than reported case data by 16 days and 10.2-fold, respectively. We made a correlation plot between the model simulated cases and the reported case data (Fig. 2C). The higher predicted number of cases and the high correlation coefficient ($R = 0.93$, $R^2 = 0.87$) imply that the model accurately captures the trend of the reported case data, while accounting for the underreported rate. This indicates that the method preserves both key properties of WBS data, which is that the trend of viral concentration in wastewater leads the trend of reported cases and can be used to estimate the true prevalence without being impacted by the underreporting rate.

In the next step, we demonstrate how the effect of temporal variation in temperature on viral loss can be incorporated in our framework. Furthermore, by incorporating the temporal effect of temperature, we can directly estimate the variation in $\gamma(T)$, the fraction of viral loss in the sewershed.

3.3. Incorporation of wastewater temperature improves model prediction

SARS-CoV-2 RNA in wastewater is subject to degradation which is affected by many factors such as temperature and travel time (Bivins et al., 2020; McCall et al., 2022). We accounted for these two factors to determine the fraction of viral decay $\gamma(T)$ in the model. Sensitivity analyses were performed to investigate how the two parameters impact model fitting. First, we tested SARS-CoV-2 degradation rates at $T_0 = 20$ °C wastewater at high titers ($\eta_0 = 0.99$ days or 23.76 hours) and low titers ($\eta_0 = 7.9$ days or 189.6 hours). Results showed a consistently better fit using viral degradation rate at low titers (Table S1). Precise estimation of the travel time is challenging given the varied flow rates and geographical distances to the wastewater treatment plant. Here, we assumed the average travel time is 18 h based on the professional experience from the treatment plant where we sampled. We also tested the sensitivity of this value by assuming 24-, 30- and 36-h travelling time and found little differences in the modeling fitting (Table S1). Viral concentration in wastewater is typically low, so we used the degradation rate at low titers and compared the die-off fraction for different temperature and travel time. Results in Table S3 showed that the viral die-off fraction differs about 5–6 fold from 10 to 30 °C.

Next, we incorporated the temporal-varying temperature data (Fig. S1) into the model framework with a travel time 18-hour and assessed model performance. By incorporating the effect of the temporal variations in temperature, the viral degradation rate also varies with temperature and time (see Materials and Methods). This temporal variation allows the model to capture the trend of clinical data with a smaller *SSE* compared to a constant degradation rate. Thus, it demonstrates the importance of incorporating temperature in our modeling framework. Additionally, the difference is statistically significant, due to one less fitting parameter, based on the corrected Akaike information criterion (Fig. 3A, B and S2) (Burnham and Anderson, 2004). We observe that the model simulation predicts an earlier peak than reported case data by 6 days, which is 10 days shorter compared to the prediction of the model without the temporal temperature effect (Fig. 3B and S2A). Additionally, the model predicts the true number of cases to be about 8.3 times higher than the reported number of cases as

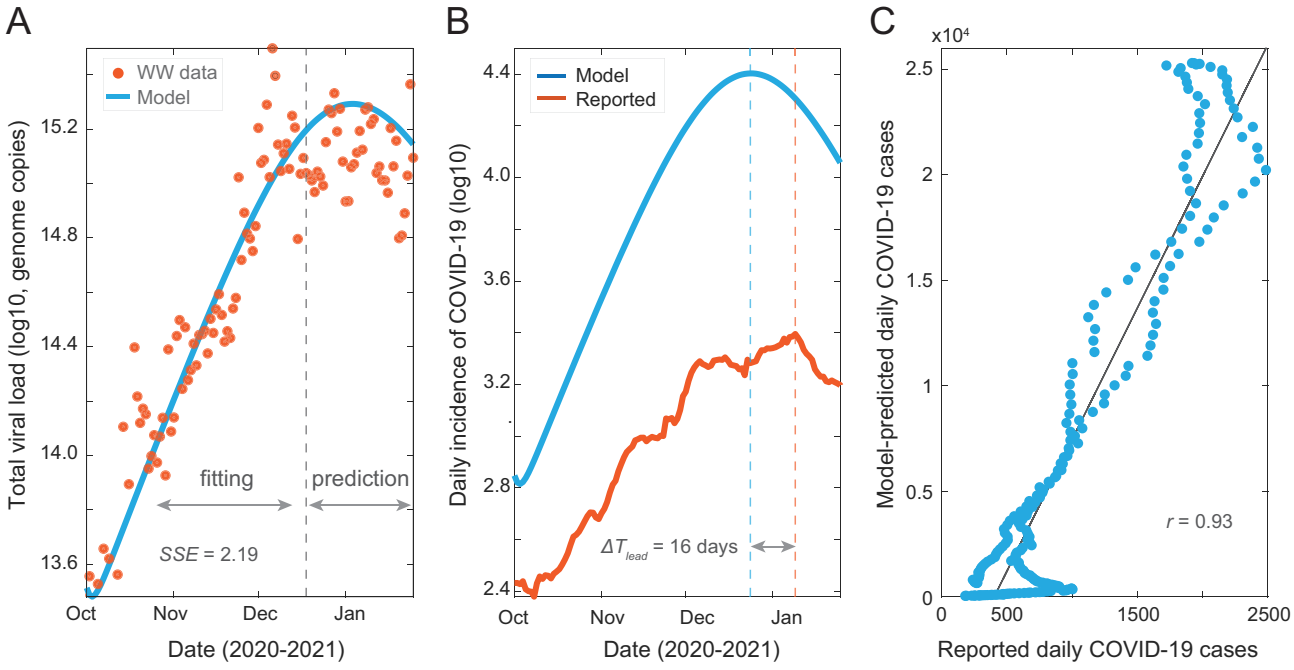

Fig. 2. Model fit and prediction to wastewater data covering the second wave of pandemic. (A) Best fit to virus concentration data in wastewater from October 2 to December 18, 2020 (dashed grey line), and model prediction to January 25, 2021. Red dots are the measured viral load in wastewater and blue curve is the modeling result. (B) Model estimation of the true number of COVID-19 cases (blue curve) and clinically reported cases (red curve). The blue and red dashed lines are dates when the two curves peak, and ΔT_{lead} is the time difference between the two peaks. (C) Correlation between simulation cases and reported cases. Best fit parameters: $\lambda = 9.66 \times 10^{-8}$ day^{-1} person^{-1}, $\alpha = 249$ *g*, $\gamma = 0.08$, and $E(0) = 11$ *people*.

Table 1
Parameters in the model.

	Definition	Unit	Value	References
S	Susceptible population	People	$S(0) = 2.3 \times 10^6$ - fixed	(Wu et al., 2022b)
E	Exposed population	People	$E(0)$ – fitting	
I	Infectious population	People	$I(0) = 0$ - fixed	
λ	Transmission rate	Per day per person	Fitting	
$1/k$	Exposed duration	Day	3 days	Wölfel et al., 2020; Killingley et al., 2022; Wu et al., 2022a; Van Kampen et al., 2021;
$1/\delta$	Infectious duration	Day	8 days	Wölfel et al., 2020, Killingley et al., 2022, Wu et al., 2022a; Van Kampen et al., 2021
α	Fecal load	Gram	51–796 g - fitting	Rose et al., 2015
β	Viral shedding in stool	Viral RNA copies per gram	Fitting	
γ	Fraction of viral loss in sewer	Per day	Fitting and estimated	
ω_1	Magnitude modifier	$\log_{10}$ viral RNA per g day	Fitting	
ω_2	Peak timing for viral shedding	Day	4 day - fixed	Killingley et al., 2022; Wu et al., 2022a.

Note that β and ω_1 are obtained from fitting to viral shedding data in stool (Wölfel et al., 2020).

compared to a predicted factor of 10.2 without the temporal effect of temperature (Fig. 3B and S2A). The predicted initial exposed population is 1182 people, which is a more reasonable estimate compared to the 11 exposed individuals predicted without the temporal effect of temperature (Fig. 3B). Those results have shown that incorporating the travel time and the temporal variation in temperature reduces the possibility of model unidentifiability and significantly improve the model performance (Table 1).

4. Discussion

Wastewater pools viral signals excreted by infected individuals across the whole spectrum of disease symptoms from asymptomatic and subclinical-symptomatic to symptomatic (Lee et al., 2020). This inclusiveness of all virus-shedding individuals offers an opportunity to better estimate the magnitude of viral infections in communities (Hart and Halden, 2020; Sanjuán and Domingo-Calap, 2021; Wu et al., 2020). However, it is challenging to convert viral concentrations in wastewater to the number of infected cases. Our group and peers previously reported methods to estimate the infection prevalence by wastewater viral load (McMahan et al., 2021; Nourbakhsh et al., 2022; Wu et al., 2020). These efforts, however, are limited because of inconsideration of dynamic viral shedding rates during the disease course and viral degradation in wastewater.

In this study, we established a quantitative framework to estimate the number of infectious COVID-19 cases and predict SARS-CoV-2 transmission through integrating wastewater surveillance data and development of an SEIR-V model. As an analogy to the four compartments of the SEIR model to simulate infectious disease dynamics at the population level, the individual-level fecal viral shedding course was divided into three periods including exposed (incubation), infectious, and recovery (Fig. 1A). The division is based on the observation that the temporal viral profiles in the nose, mouth, and stool are strikingly similar qualitatively with high viral

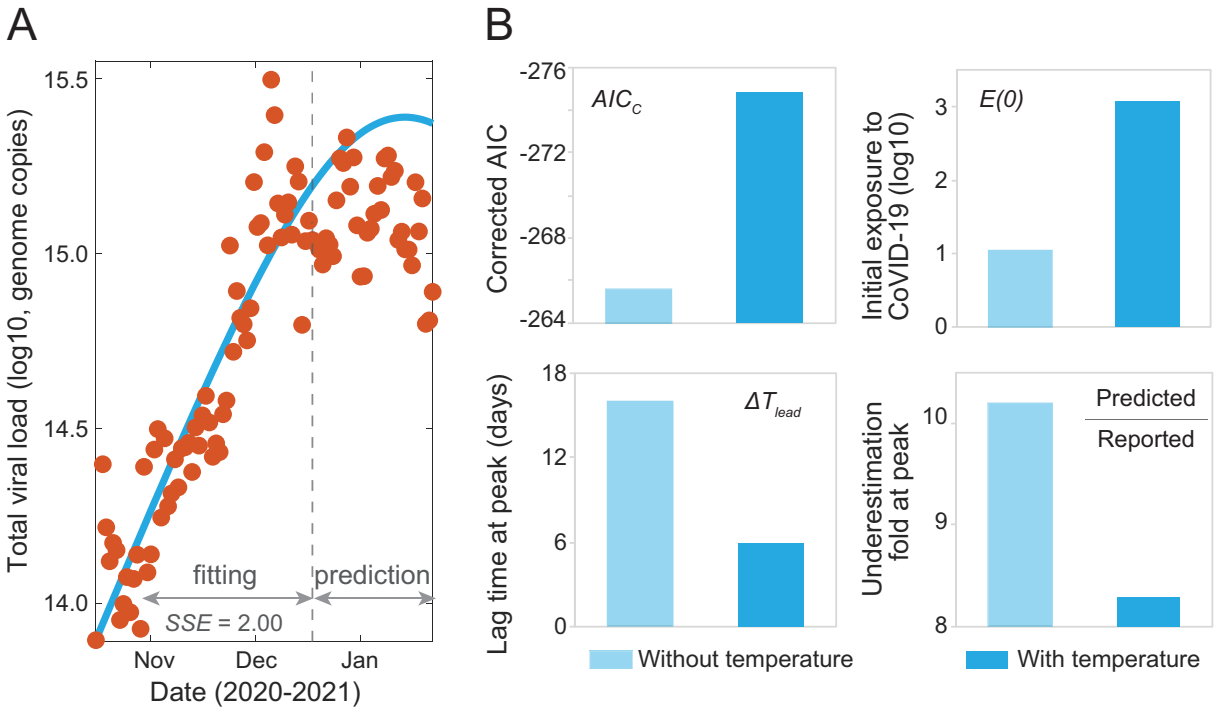

Fig. 3. Incorporating the effect of temporal variation of wastewater temperature in the SEIR-V model. (A) Best fit to viral concentration data in wastewater from October 2 to December 18, 2020 (dashed grey line), and model prediction to January 25, 2021. Red dots are the measured viral load in wastewater and blue curve is the modeling result. (B) Comparison of the SEIR-V models with and without incorporating temperature effect. Top left: corrected Akaike information criterion (*AICc*) values, the statistically significant *AICc* difference is 9.2; Top right: initial populations exposed to SARS-CoV-2; Bottom left: wastewater lead time difference at peak; Bottom right: fold of difference between the number of predicted cases and clinically reported cases. The AIC/AICc are calculated assuming normal distribution of residuals with mean zero using the formulas $AIC = n \log\left(\frac{sse}{n}\right) + 2k$ and $AICc = AIC + \frac{2k(k+1)}{n-k-1}$, where n is the number of data used for fitting, k is the number of fitting parameter and the SSE is calculated based on the data used for fitting. Light blue represents the model without including temperate effect, while blue represents the model with temperature effect. Best fit parameters when incorporating temperature: $\lambda = 9.06 \times 10^{-8}$ day^{-1} person^{-1}, $\alpha = 360$ *g*,and $E(0) = 1182$ people.

load associated with infectiousness (Killingley et al., 2022; Wölfel et al., 2020). With this concept, we estimated the population-level average viral shedding rate during the infectious phase using clinically reported SARS-CoV-2 concentrations in hospitalized patients' stool samples (Fig. 1B). This estimated viral shedding rate is an average of infected individuals in the population and does not consider the heterogenous viral shedding dynamics among infected individuals (Wölfel et al., 2020; Killingley et al., 2022; Stanca and Tuncer et al., 2022). Thus, our model can be improved by including viral shedding data during the early phase of the infection and large-scale individual-level shedding dynamics data.

It is noteworthy to mention that the "*I*" in the SEIR model is the "infectious" class, not the "infected" class. This contrasts with the conventional approaches that use mean or median viral shedding rate in a group of tested samples regardless of the phase of the infection (Saththasivam et al., 2021; Petala et al., 2022; Schmitz et al., 2021). By focusing on the infectious population, which is also the main contributor of viral shedding in wastewater, we greatly simplify the typical complex structure of the SEIR-type models that implement WBS (Fig. S3) and reduce the likelihood of model unidentifiability.

By fitting an SEIR-V model to wastewater data within our framework, we show that the method retains key advantages of using wastewater. Specifically, the inferred case data from the best fit parameters leads the reported case data by 6–16 days and implies a large ratio (8.3–10.2) of true prevalence to clinically reported cases, which are consistent with previous results (Wu et al., 2020; Wu et al., 2022a; Eikenberry et al., 2020; Angulo et al., 2021). We also incorporate the important effects of temperature with temporal variations and travel time on the viral degradation rate in a simple manner that is applicable to a larger time scale. We note that extension to incorporate time-dependent variations of the fecal viral shedding rate within this framework is straightforward but will require careful consideration for the convergence of the numerical method. Together, our work shows the potential and flexibility of the framework to incorporate WBS in epidemic models.

The foundation of our framework is independent of the epidemic model formulation, yet its application depends greatly on the epidemic models for specific situations. For example, if we want to apply the framework to capture a period with significant changes to social behavior, perhaps due to the effect of a social intervention, then an appropriate change to the structure of the SEIR model to reflect these structures is necessary (Johnston and Pell, 2020; Fenichel et al., 2011; Pell et al., 2018). However, if multiple variants are of interest, then the SEIR model itself needs to be extended to a multi-variant version and incorporate known biological properties of different variants (Dyson et al., 2021; Gonzalez-Parra et al., 2021). Similarly, interventions (such as vaccination) and the impact of social gatherings must first be included in the epidemic model prior to its integration within our framework (Saad-Roy et al., 2021; Giordano et al., 2021; Buckner et al., 2021; Makhoul et al., 2020).

Our modeling framework represents a simplified picture that describes the connection between viral transmission in the human population and viral concentration in wastewater. For this demonstrative purpose, we make various simplifying assumptions that would need to be adjusted for application of the framework to specific situations. Firstly, the SEIR model assumes a completely susceptible, homogenous, and well-mixed population. In practice, specific contacting/population structure of the region being studied must be taken into account to provide accurate estimates of relevant epidemiological quantities, such as the basic or effective reproduction number. Secondly, we assume that the viral concentration in wastewater is contributed mainly by the infectious group. A direct calculation of the respective viral contribution from each group, assuming a cut-off threshold of 2 log using the best estimate of the viral shedding function $f(t)$ gives 12 % , 52% and 36% relative contribution from *E*, *I* and *R* classes, respectively. Taking this into account would roughly reduce the fold-difference between predicted and reported cases by about 50 %. A simple approach would be to consider the contribution from the *E* and *R* classes similar to that of the *I* class (e.g., by finding the average viral shedding rate β for each class). Alternatively, a convolution of $f(t)$ and everyone who has ever been infected can also be done to account for the ever-changing viral shedding rate. However, such a model would need to reconcile the differences between the temporal variations in the fecal viral shedding and infectiousness. This can be done by studying the relationship between viral dynamics in the stool and the nose or throat. Finally, while we only consider the effects of temperature and travel time on viral decay rate, other in-sewer factors, such as organic matter, particles, pH, solvents, detergents, and microbes could also affect the viral die-off fractions and should be considered when appropriate (Bertels et al., 2022; Chahal et al., 2016; Gundy et al., 2009).

Dynamical epidemic models are useful tools to track pandemic progression and to assess the potential impact of hypothetical situations such as stay-at-home orders or the emergence of a resistant viral strain. However, sparsely reported case data with high uncertainty, due partially to the high underreporting rate, can compromise the ability of epidemic models to provide an accurate forecast of the pandemic and limit their application to retrospective studies. Hence, WBS, which bypasses both the tremendous difficulty in data collection faced by the standard clinical reporting practice and the high underreporting rate, represents a potential solution to address this challenge faced by the modeling community. WBS data also provides a leading indicator of the pandemic progression and is not limited to SARS-CoV-2, thus it can further enhance the prediction and applicability of epidemic models for public health purposes. Together, this aspect of our framework highlights the importance of interdisciplinary collaboration to better address public health concerns.

5. Conclusions

In this study, we have established a quantitative framework to estimate COVID-19 prevalence and predict SARS-CoV-2 transmission by incorporating WBS data in a simple epidemic SEIR-V model. The main conclusions are:

- We constructed a simple and effective framework to incorporate WBS data to epidemic models. The developed SEIR-V model captures the temporal dynamics of clinical COVID-19 cases and preserves key advantages of WBS data over reported case data.
- We illustrated how the effect of travel time and temperature on viral decay can be incorporated within our framework to improve model performance and robustness, which is an important component to model disease transmission in real world applications.
- The modeling framework is a valuable platform to integrate WBS with epidemic models to provide accurate and robust estimates of the pandemic progression and examine the potential impact of interventions to inform public health decision making.

CRediT authorship contribution statement

Tin Phan: Conceptualization; Methodology; Formal analysis; Writing - Original Draft; Visualization; Writing - review & editing;

Samantha Brozak: Conceptualization; Methodology; Formal analysis; Writing - review & editing;

Bruce Pell: Conceptualization; Methodology; Formal analysis; Writing - review & editing;

Anna Gitter: Discussion; Writing - review & editing.

Amy Xiao: Discussion; Writing - review & editing.

Kristina D. Mena: Discussion; Writing - review & editing.

Yang Kuang: Conceptualization; Methodology; Funding acquisition; Formal analysis; Writing - review & editing; Supervision.

Fuqing Wu: Conceptualization; Methodology; Funding acquisition; Formal analysis; Visualization; Writing - Original Draft; Writing - review & editing; Supervision.

Data availability

The data and code are provided in the supplementary materials

Declaration of competing interest

The authors declare that they have no known competing financial interests or personal relationships that could have appeared to influence the work reported in this paper.

Acknowledgement

This work is supported by Faculty Startup funding from the Center of Infectious Diseases at UTHealth, the UT system Rising STARs award, and the Texas Epidemic Public Health Institute (TEPHI) to F.W. This work was also supported by Director's postdoctoral fellowship at Los Alamos National Laboratory to T.P.; Y.K. and S.B. are partially supported by the US National Science Foundation Rules of Life program DEB -1930728 and the NIH grant 5R01GM131405-02.

Appendix A. Supplementary data

Supplementary data to this article can be found online at https://doi.org/10.1016/j.scitotenv.2022.159326.

References

Angulo, Frederick J., Finelli, Lyn, Swerdlow, David L., 2021. Estimation of US SARS-CoV-2 infections, symptomatic infections, hospitalizations, and deaths using seroprevalence surveys. JAMA Netw. Open 4 (1), 2033706.
B˝ehrádek, J., 1930. Temperature coefficients in biology. Biol. Rev. 5 (1), 30–58.
Bertels, Xander, et al., 2022. Factors influencing SARS-CoV-2 RNA concentrations in wastewater up to the sampling stage: a systematic review. Sci. Total Environ. 153290.
Bivins, Aaron, et al., 2020. Persistence of SARS-CoV-2 in water and wastewater. Environ.Sci. Technol.Lett. 7 (12), 937–942.
Boucau, Julie, et al., 2022. Duration of shedding of culturable virus in SARS-CoV-2 Omicron (BA. 1) infection. N. Engl. J. Med. 387 (3), 275–277.
Brouwer, Andrew F., et al., 2022. The role of time-varying viral shedding in modelling environmental surveillance for public health: revisiting the 2013 poliovirus outbreak in Israel. J. R. Soc. Interface 19 (190), 20220006.
Brozak, Samantha J., Mohammed-Awel, Jemal, Gumel, Abba B., 2022. Mathematics of a single-locus model for assessing the impacts of pyrethroid resistance and temperature on population abundance of malaria mosquitoes. Infect.Dis.Model. 7 (3), 277–316.
Buckner, Jack H., Chowell, Gerardo, Springborn, Michael R., 2021. Dynamic prioritization of COVID-19 vaccines when social distancing is limited for essential workers. Proc. Natl. Acad. Sci. 118 (16), 2025786118.
Burnham, Kenneth P., Anderson, David R., 2004. Multimodel inference: understanding AIC and BIC in model selection. Sociol. Methods Res. 33 (2), 261–304.
CDC, 2020. National Wastewater Surveillance System. Centers for Disease Control and Prevention.
CDC, 2022. Ending Isolation and Precautions for People with COVID-19: Interim Guidance. Centers for Disease Control and Prevention.
CDC, 2022. Symptoms of COVID-19. Center for Disease Control and Prevention.
Chahal, C., van den Akker, B., Young, F., Franco, C., Blackbeard, J., Monis, P., 2016. Chapter two - pathogen and particle associations in wastewater: significance and implications for treatment and disinfection processes. In: Sariaslani, S., Michael Gadd, G. (Eds.), Advances in Applied Microbiology. Academic Press, pp. 63–119 https://doi.org/10.1016/bs.aambs.2016.08.001.
Ciupe, S.M., Tuncer, N., 2022. Identifiability of parameters in mathematical models of SARS-CoV-2 infections in humans. Sci. Rep. 12, 14637. https://doi.org/10.1038/s41598-022-18683-x.
Dyson, Louise, et al., 2021. Possible future waves of SARS-CoV-2 infection generated by variants of concern with a range of characteristics. Nat. Commun. 12 (1), 1–13.
Eikenberry, Steffen E., et al., 2020. To mask or not to mask: modeling the potential for face mask use by the general public to curtail the COVID-19 pandemic. Infect.Dis.Model. 5, 293–308.
Eisenberg, Marisa C., et al., 2013. Identifiability and estimation of multiple transmission pathways in cholera and waterborne disease. J. Theor. Biol. 324, 84–102.
Fenichel, Eli P., et al., 2011. Adaptive human behavior in epidemiological models. Proc. Natl. Acad. Sci. 108 (15), 6306–6311.
Ferretti, Luca, et al., 2020. Quantifying SARS-CoV-2 transmission suggests epidemic control with digital contact tracing. Science 368 (6491), eabb6936.
Giordano, Giulia, et al., 2021. Modeling vaccination rollouts, SARS-CoV-2 variants and the requirement for non-pharmaceutical interventions in Italy. Nat. Med. 27 (6), 993–998.
Gonzalez-Parra, Gilberto, Martínez-Rodríguez, David, Villanueva-Micó, Rafael J., 2021. Impact of a new SARS-CoV-2 variant on the population: a mathematical modeling approach. Math.Comput.Appl. 26 (2), 25.
Guan, Wei-Jie, et al., 2020. Clinical characteristics of coronavirus disease 2019 in China. N. Engl. J. Med. 382 (18), 1708–1720.
Gundy, P.M., Gerba, C.P., Pepper, I.L., 2009. Survival of coronaviruses in water and wastewater. Food Environ. Virol. 1, 10. https://doi.org/10.1007/s12560-008-9001-6.
Han, M.S., et al., 2020. Viral RNA load in mildly symptomatic and asymptomatic children with COVID-19, Seoul, South Korea. Emerg. Infect. Dis. 2497.
Hart, O.E., Halden, R.U., 2020. Computational analysis of SARS-CoV-2/COVID-19 surveillance by wastewater-based epidemiology locally and globally: feasibility, economy, opportunities and challenges. Sci. Total Environ. 730, 138875.
He, Xi, et al., 2020. Temporal dynamics in viral shedding and transmissibility of COVID-19. Nat. Med. 26 (5), 672–675.
Heitzman-Breen, Nora, Ciupe, Stanca M., 2022. Modeling within-host and aerosol dynamics of SARS-CoV-2: the relationship with infectiousness. PLoS Comput. Biol. 18 (8), e1009997.
Johnston, Matthew D., Pell, Bruce, 2020. A dynamical framework for modeling fear of infection and frustration with social distancing in COVID-19 spread. Math. Biosci. Eng. 17 (6), 7892–7915.
Jones, David L., et al., 2020. Shedding of SARS-CoV-2 in feces and urine and its potential role in person-to-person transmission and the environment-based spread of COVID-19. Sci. Total Environ. 749, 141364.
Kampen, Van, et al., 2021. Duration and key determinants of infectious virus shedding in hospitalized patients with coronavirus disease-2019 (COVID-19). Nat. Commun. 12 (1), 1–6.
Karthikeyan, Smruthi, et al., 2022. Wastewater sequencing reveals early cryptic SARS-CoV-2 variant transmission. Nature 1–4.
Ke, Ruian, et al., 2021. In vivo kinetics of SARS-CoV-2 infection and its relationship with a person's infectiousness. Proc. Natl. Acad. Sci. 118 (49).
Ke, Ruian, et al., 2022. Daily longitudinal sampling of SARS-CoV-2 infection reveals substantial heterogeneity in infectiousness. Nat. Microbiol. 7 (5), 640–652.
Killingley, et al., 2022. Safety, tolerability and viral kinetics during SARS-CoV-2 human challenge in young adults. Nat. Med. 28 (5), 1031–1041.
Krivoňáková, N., et al., 2021. Mathematical modeling based on RT-qPCR analysis of SARS-CoV-2 in wastewater as a tool for epidemiology. Sci. Rep. 11 (1), 1–10.
Lauer, Stephen A., et al., 2020. The incubation period of coronavirus disease 2019 (COVID-19) from publicly reported confirmed cases: estimation and application. Ann. Intern. Med. 172 (9), 577–582.
Lee, S., et al., 2020. Clinical course and molecular viral shedding among asymptomatic and symptomatic patients with SARS-CoV-2 infection in a community treatment center in the Republic of Korea. JAMA Intern. Med. 180, 1447–1452.
Li, Qun, et al., 2020. Early transmission dynamics in Wuhan, China, of novel coronavirus-infected pneumonia. N. Engl. J. Med. 382, 1199–1207.
Makhoul, et al., 2020. Epidemiological impact of SARS-CoV-2 vaccination: mathematical modeling analyses. Vaccines 8 (4), 668.
Mccall, Camille, et al., 2022. Modeling SARS-CoV-2 RNA degradation in small and large sewersheds. Environ.Sci.Water Res.Technol. 8 (2), 290–300.
McMahan, C.S., et al., 2021. COVID-19 wastewater epidemiology: a model to estimate infected populations. Lancet Planet.Health 2021 (5), e874–e881.
Naughton, Colleen C., et al., 2021. Show Us the Data: Global COVID-19 Wastewater Monitoring Efforts, Equity, and Gaps. MedRXiv.
Nourbakhsh, Shokoofeh, et al., 2022. A wastewater-based epidemic model for SARS-CoV-2 with application to three Canadian cities. Epidemics 39, 100560.
Peccia, Jordan, et al., 2020. Measurement of SARS-CoV-2 RNA in wastewater tracks community infection dynamics. Nat. Biotechnol. 38 (10), 1164–1167.
Pell, Bruce, et al., 2018. Simple multi-scale modeling of the transmission dynamics of the 1905 plague epidemic in Bombay. Math. Biosci. 301, 83–92.
Petala, Maria, et al., 2022. Relating SARS-CoV-2 shedding rate in wastewater to daily positive tests data: a consistent model based approach. Sci. Total Environ. 807, 150838.
Proverbio, Daniele, et al., 2022. Model-based assessment of COVID-19 epidemic dynamics by wastewater analysis. Sci. Total Environ. 827, 154235.
Randazzo, W., et al., 2020. SARS-CoV-2 RNA in wastewater anticipated COVID-19 occurrence in a low prevalence area. Water Res. 181, 115942.
Reyes, Bryan A., Pendergast, Julie S., Yamazaki, Shin, 2008. Mammalian peripheral circadian oscillators are temperature compensated. J. Biol. Rhythm. 23 (1), 95–98.
Rose, C., et al., 2015. The characterization of feces and urine: a review of the literature to inform advanced treatment technology. Crit. Rev. Environ. Sci. Technol. 45 (17), 1827–1879.
Saad-Roy, et al., 2021. Epidemiological and evolutionary considerations of SARS-CoV-2 vaccine dosing regimes. Science 372 (6540), 363–370.
Safford, H.R., Shapiro, K., Bischel, H.N., 2022. Wastewater analysis can be a powerful public health tool—if it's done sensibly. Proc. Nat. Acad. Sci. 119 (6), e2119600119.
Saguti, Fredy, et al., 2021. Surveillance of wastewater revealed peaks of SARS-CoV-2 preceding those of hospitalized patients with COVID-19. Water Res. 189, 116620.
Sanjuán, R., Domingo-Calap, P., 2021. Reliability of wastewater analysis for monitoring COVID-19 incidence revealed by a long-term follow-up study. Front. Virol. 1.
Saththasivam, et al., 2021. COVID-19 (SARS-CoV-2) outbreak monitoring using wastewater-based epidemiology in Qatar. Sci. Total Environ. 774, 145608.
Schmitz, W., et al., Bradley, 2021. Enumerating asymptomatic COVID-19 cases and estimating SARS-CoV-2 fecal shedding rates via wastewater-based epidemiology. Sci. Total Environ. 801, 149794.
Tuncer, Necibe, et al., 2022. Parameter identifiability and optimal control of an SARS-CoV-2 model early in the pandemic. J. Biol. Dyn. 16 (1), 412–438.
Wölfel, Roman, et al., 2020. Virological assessment of hospitalized patients with COVID-2019. Nature 581 (7809), 465–469.
Wu, F., Lee, W.L., et al., 2022b. Making waves: wastewater surveillance of SARS-CoV-2 in an endemic future. Water Res. 118535.
Wu, Fuqing, Xiao, Amy, et al., 2022a. SARS-CoV-2 RNA concentrations in wastewater foreshadow dynamics and clinical presentation of new COVID-19 cases. Sci. Total Environ. 805, 150121.
Wu, Fuqing, et al., 2020. SARS-CoV-2 titers in wastewater are higher than expected from clinically confirmed cases. mSystems 2020 (5), e00614-20.
Wu, Zhimin, et al., 2019. Predictability and identifiability assessment of models for prostate cancer under androgen suppression therapy. Math. Biosci. Eng. 16 (5), 3512–3536.
Xiao, Amy, et al., 2022. Metrics to relate COVID-19 wastewater data to clinical testing dynamics. Water Res. 118070.